

# High-Redshift Cosmography

---

**Vincenzo Vitagliano<sup>1,2</sup>, Jun-Qing Xia<sup>1</sup>, Stefano Liberati<sup>1,2</sup>, Matteo Viel<sup>2,3</sup>**

<sup>1</sup>*SISSA, Via Beirut 2-4, 34151 Trieste, Italy*

<sup>2</sup>*INFN sez. Trieste, Via Valerio 2, 34127 Trieste, Italy*

<sup>3</sup>*INAF-Osservatorio Astronomico di Trieste, Via G.B. Tiepolo 11, I-34131 Trieste, Italy*

*Email: vitaglia@sissa.it, xia@sissa.it, liberati@sissa.it, viel@oats.inaf.it*

**ABSTRACT:** We constrain the parameters describing the kinematical state of the universe using a cosmographic approach, which is fundamental in that it requires a very minimal set of assumptions (namely to specify a metric) and does not rely on the dynamical equations for gravity. On the data side, we consider the most recent compilations of Supernovae and Gamma Ray Bursts catalogs. This allows to further extend the cosmographic fit up to  $z = 6.6$ , i.e. up to redshift for which one could start to resolve the low  $z$  degeneracy among competing cosmological models. In order to reliably control the cosmographic approach at high redshifts, we adopt the expansion in the improved parameter  $y = z/(1+z)$  (as proposed in Class. Quant. Grav. **24** (2007) 5985). This series has the great advantage to hold also for  $z > 1$  and hence it is the appropriate tool for handling data including non-nearby distance indicators. We find that Gamma Ray Bursts, probing higher redshifts than Supernovae, have constraining power and do require (and statistically allow) a cosmographic expansion at higher order than Supernovae alone. Exploiting the set of data from Union and GRBs catalogues, we show for the first time a definitively negative deceleration parameter  $q_0$  up to the  $3\sigma$  confidence level. We present also forecasts for realistic data sets that are likely to be obtained in the next few years.

---

## Contents

<b>1. Introduction</b>	<b>1</b>
<b>2. Supernovae and GRB Datasets</b>	<b>4</b>
<b>3. Statistical Analysis</b>	<b>5</b>
3.1 Cosmography I	5
3.2 Cosmography II	7
3.3 Summary	10
<b>4. Future Perspectives</b>	<b>11</b>
<b>5. Conclusions</b>	<b>12</b>

---

## 1. Introduction

A huge amount of cosmological data sets with increasing reliability has been collected during the last decade, providing new insights on the dynamical state of our universe. The interpretation of the Hubble diagram for Type Ia Supernovae (SNeIa) and the observations of polarization and anisotropies in the power spectrum of the Cosmic Microwave Background (CMB) showed that the universe is undergoing an accelerated phase of expansion. Furthermore, the availability of new cosmological probes, such as high redshift SNe and Gamma-Ray Bursts (GRBs), enables to improve the knowledge of the cosmological parameters and allows to distinguish among different models: any new test should be a challenge for all the attempts providing an explanation of the current cosmic acceleration. On the other hand, a recent recovery of a model independent approach (the cosmographic one [1, 2]) gained increasing interest for catching as much information as possible directly from observations, retaining the minimal priors of isotropy and homogeneity and leaving aside any other assumption. Let us stress that the idea supporting cosmography is rather clean: here we are not providing any new model for Dark Energy, but just a deeper, even if simpler, analysis of the cosmological data sets with the aim to give a fiducial frame against which any theoretical proposal should be tested. The only ingredient taken into account *a priori* is the FLRW line element obtained from kinematical requirements

$$ds^2 = -c^2 dt^2 + a^2(t) \left[ \frac{dr^2}{1 - kr^2} + r^2 d\Omega^2 \right] ; \quad (1.1)$$

exploiting this metric, it is possible to express the luminosity distance  $d_L$  as a power series in the redshift parameter  $z$ , the coefficients of the expansion being functions of the scale factor  $a(t)$  and its higher order derivatives.

In this paper we will discuss the use of luminosity distance indicators in the high redshift universe in order to constrain the values of fundamental cosmological parameters that describe the model we are interested in.

Even though the prominent role of SNe (in the high- $z$  version, too) in doing the job is well-known, the potentiality of GRBs as cosmological standard candles has been recently explored as a possible proposal to increase the number of high redshift distance ladders. Data coming from observations of both SNe and GRBs are used to fit directly the expression for the luminosity distance  $d_L$ .

Following [3],  $d_L$  can be defined from the relation between the apparent luminosity  $l$  of an object and its absolute luminosity  $L$

$$l = \frac{L}{4\pi r_1^2 a^2(t_0)(1+z)^2} = \frac{L}{4\pi d_L^2}, \quad (1.2)$$

where  $r_1$  is the comoving radius of the light source emitting at time  $t_1$ ,  $t_0$  is the later time an observer in  $r = 0$  is catching the photons, and redshift  $z$  is, as usual, defined as  $1+z = a(t_0)/a(t_1)$ . The radial coordinate  $r_1$  in a FLRW universe can be written for small distances as [4]

$$r_1 = \int_{t_1}^{t_0} \frac{c}{a(t)} dt - \frac{k}{3!} \left[ \int_{t_1}^{t_0} \frac{c}{a(t)} dt \right]^3 + \mathcal{O}(5), \quad (1.3)$$

with  $k = -1, 0, +1$  respectively for hyperspherical, Euclidean or spherical universe. In such a way, it is possible to recover the expansion of  $d_L$  for small  $z$

$$d_L(z) = cH_0^{-1} \left\{ z + \frac{1}{2}(1-q_0)z^2 - \frac{1}{6} \left( 1 - q_0 - 3q_0^2 + j_0 + \frac{kc^2}{H_0^2 a^2(t_0)} \right) z^3 + \right. \\ \left. + \frac{1}{24} \left[ 2 - 2q_0 - 15q_0^2 - 15q_0^3 + 5j_0 + 10q_0j_0 + s_0 + \frac{2kc^2(1+3q_0)}{H_0^2 a^2(t_0)} \right] z^4 + \dots \right\}, \quad (1.4)$$

having defined the cosmographic parameters as:

$$H_0 \equiv \frac{1}{a(t)} \frac{da(t)}{dt} \Big|_{t=t_0} \equiv \frac{\dot{a}(t)}{a(t)} \Big|_{t=t_0}, \quad (1.5)$$

$$q_0 \equiv -\frac{1}{H^2} \frac{1}{a(t)} \frac{d^2 a(t)}{dt^2} \Big|_{t=t_0} \equiv -\frac{1}{H^2} \frac{\ddot{a}(t)}{a(t)} \Big|_{t=t_0}, \quad (1.6)$$

$$j_0 \equiv \frac{1}{H^3} \frac{1}{a(t)} \frac{d^3 a(t)}{dt^3} \Big|_{t=t_0} \equiv \frac{1}{H^3} \frac{a^{(3)}(t)}{a(t)} \Big|_{t=t_0}, \quad (1.7)$$

$$s_0 \equiv \frac{1}{H^4} \frac{1}{a(t)} \frac{d^4 a(t)}{dt^4} \Big|_{t=t_0} \equiv \frac{1}{H^4} \frac{a^{(4)}(t)}{a(t)} \Big|_{t=t_0}. \quad (1.8)$$

It is important to stress the existence of other definitions for distance indicators [2] rather than the more often used  $d_L$ : depending on which physical quantity one is measuring, it could be more convenient to extract from data one of these instead of the luminosity distance. These different quantities admit different expressions of the Taylor expansion in the redshift, such that it could be more natural to estimate cosmographic parameters, whose

expression instead does not depend on the analytic expansion, in one of these particular frameworks. This ambiguity could lead to a misunderstanding even about the proper definition of distance one should retain. From now on we will refer only to luminosity distance since it is the most direct choice in the case of measures of distance for SNe and GRBs.

In two recent works the authors of [5], have performed a first attempt to fit luminosity distance by data using more distant objects as “standard candles”, however, the ill-behavior at high  $z$  of the redshift expansion used there strongly affected the results. We are no longer going to use the standard relation linking the luminosity distance to the ordinary-defined redshift. As already pointed out in [1], the lack of validity of the Taylor-expanded expression for  $d_L$  could be settled down approximately at  $z \sim 1$ . In order to avoid problems with the convergence of the series for the highest redshift objects as well as to control properly the approximation induced by truncations of the expansions, it is useful to recast  $d_L$  as a function of an improved parameter  $y = z/(1+z)$ . In such a way, being  $z \in (0, \infty)$  mapped into  $y \in (0, 1)$ , we will be in principle able to retrieve the right behaviour for series convergence at any distance. The introduction of this new redshift variable will not affect the definition of cosmographic parameters, while the luminosity distance at fourth order in the  $y$ -parameter becomes:

$$d_L(y) = \frac{c}{H_0} \left\{ y - \frac{1}{2}(q_0 - 3)y^2 + \frac{1}{6} [12 - 5q_0 + 3q_0^2 - (j_0 + \Omega_0)] y^3 + \frac{1}{24} [60 - 7j_0 - 10\Omega_0 - 32q_0 + 10q_0j_0 + 6q_0\Omega_0 + 21q_0^2 - 15q_0^3 + s_0] y^4 + \mathcal{O}(y^5) \right\}, \quad (1.9)$$

where  $\Omega_0 = 1 + kc^2/H_0^2 a^2(t_0)$  is the total energy density. For the flat universe,  $\Omega_0 = 1$ . On the other hand, luminosity distance can also be expressed as “logarithmic Hubble relations”:

$$\ln \left[ \frac{d_L(y)}{y \text{ Mpc}} \right] = \frac{\ln 10}{5} [\mu(y) - 25] - \ln y = \ln \left[ \frac{c}{H_0} \right] - \frac{1}{2}(q_0 - 3)y + \frac{1}{24} [21 - 4(j_0 + \Omega_0) + q_0(9q_0 - 2)] y^2 + \frac{1}{24} [15 + 4\Omega_0(q_0 - 1) + j_0(8q_0 - 1) - 5q_0 + 2q_0^2 - 10q_0^3 + s_0] y^3 + \mathcal{O}(y^4); \quad (1.10)$$

and then, the distance modulus (in which are expressed current data) is given by the expression:

$$\mu(y) = 25 + \frac{5}{\ln 10} \left\{ \ln \left[ \frac{c}{H_0} \right] + \ln y - \frac{1}{2}(q_0 - 3)y + \frac{1}{24} [21 - 4(j_0 + \Omega_0) + q_0(9q_0 - 2)] y^2 + \frac{1}{24} [15 + 4\Omega_0(q_0 - 1) + j_0(8q_0 - 1) - 5q_0 + 2q_0^2 - 10q_0^3 + s_0] y^3 + \mathcal{O}(y^4) \right\}. \quad (1.11)$$

It is clear that the higher the order reached in the redshift expansion of  $d_L$ , the better the data fitting will be (more free parameters). However, for a given a data set there will be an upper bound on the order of the expansion which is statistically significant in fitting the data. In the following sections we shall fit the data with two different truncations of expansion (1.10) without and with the third order term ( $y^3$ ). For the sake of conciseness

we shall respectively label them as Cosmography I and Cosmography II. While we shall see that the higher redshift data make the latter truncation the most statistically significant among the two, we shall show in the end that no improvement is at the moment achievable by extending the truncation to fourth order in  $y$ .

## 2. Supernovae and GRB Datasets

The SNIa distance moduli provide the luminosity distance as a function of redshift. In this paper we will use two different SNIa datasets: one is the SuperNova Legacy Survey (SNLS) data over a redshift range  $z = 0 - 1$  which consists of 115 data points [6], and the other one is the recently released Union compilation (307 data points) from the Supernova Cosmology project [7], which include the recent samples of SNIa from the SNLS and ESSENCE survey, as well as some older data sets, and span the redshift range  $0 \lesssim z \lesssim 1.55$ . We do not include the data from CfA as their reliability is controversial [8] and in any case, being extremely low redshift ( $z < 0.1$ ), they would not affect the high  $z$  behaviour which is the main trust of our investigation.

In addition, we consider GRBs that can potentially be used to measure the luminosity distance out to higher redshift than SNIa. GRBs are not standard candles since their isotropic equivalent energetics and luminosities span 3-4 orders of magnitude. However, similarly to SNIa it has been proposed to use correlations between various properties of the prompt emission and also of the afterglow emission to standardize GRB energetics (e.g. [17]). Recently, several empirical correlations between GRB observables were reported, and these findings have triggered intensive studies on the possibility of using GRBs as cosmological “standard” candles (Ref. [5], *e.g.*, finds the cosmographic parameters from luminosity distance data obtained exploiting different relations among GRBs quantities.).

For example, the GRB isotropic luminosities can be computed as a function of redshift using the bolometric fluence and the two exhibit strong correlations with the rest frame peak energy. However, due to the lack of low-redshift long GRBs data to calibrate these relations, in a cosmology-independent way, the parameters of the reported correlations are given assuming an input cosmology and obviously depend on the same cosmological parameters that we would like to constrain. Thus, applying such relations to constrain cosmological parameters leads to biased results.

In Ref. [10] this “circular problem” is naturally eliminated by marginalizing over the free parameters involved in the correlations; in addition, some results show that these correlations do not change significantly for a wide range of cosmological parameters [11, 12]. Therefore, in this paper we use the 69 GRBs over a redshift range from  $z = 0.17 - 6.60$  presented in Ref. [12], but we keep in mind the issues related to the circular problem that are more extensively discussed in Ref. [10] and also the fact that all the correlations used to standardize GRBs have scatter and are poorly understood under the physical point of view. For a more extensive discussion and for a full presentation of a GRB Hubble Diagram with the same sample that we used we refer the reader to Section 4 of Ref. [12].

In the calculation of the likelihood from SNIa and GRBs, which will be presented in the next sections, we have marginalized over the absolute magnitude  $M$  which is a nuisance

parameter, as done in Ref. [13]:

$$\bar{\chi}^2 = A - \frac{B^2}{C} + \ln \left( \frac{C}{2\pi} \right) , \quad (2.1)$$

where

$$A = \sum_i \frac{(\mu^{\text{data}} - \mu^{\text{th}})^2}{\sigma_i^2} , \quad B = \sum_i \frac{\mu^{\text{data}} - \mu^{\text{th}}}{\sigma_i^2} , \quad C = \sum_i \frac{1}{\sigma_i^2} . \quad (2.2)$$

In order to compute the likelihood, we use a Monte Carlo Markov Chain technique as it is usually done in order to explore efficiently a multi-dimensional parameter space in a Bayesian framework (this procedure has been used only when the number of parameters becomes larger than three, otherwise direct calculation of the likelihood has been performed).

### 3. Statistical Analysis

In this section we present our main results on the constraints for the cosmographic expansion from the current observational data sets.

#### 3.1 Cosmography I

Firstly, we use the polynomial series of the logarithmic Hubble relation up to second order, namely Cosmography I. In this case, there are two free parameters: the deceleration  $q_0$  and the jerk parameter  $j_0 + \Omega_0$ . In Fig. 1 we show the one dimensional likelihood distributions for these parameters as obtained from different data combinations. Using the SNLS data

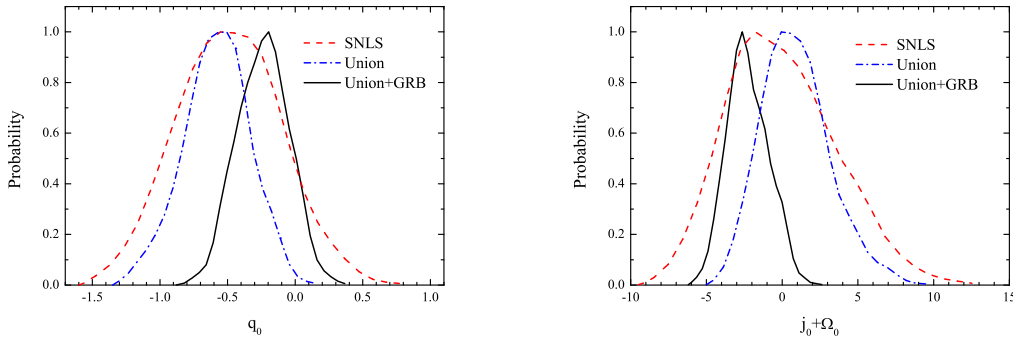


**Figure 1:** One-dimensional likelihood distributions for the parameters  $q_0$  and  $j_0 + \Omega_0$  from different data combinations in the Cosmography I case: SNLS (red dashed lines), Union (blue dash-dot lines) and Union+GRB (black solid lines).

only, we obtain the constraints on  $q_0$  and  $j_0 + \Omega_0$  at 68% confidence level ( $1 \sigma$ ):

$$q_0 = -0.49 \pm 0.38 , \quad j_0 + \Omega_0 = -0.52 \pm 3.52 , \quad (3.1)$$

which is consistent with the previous work [2]. Furthermore, the Union dataset gives more stringent  $1\sigma$  constraints on the parameters:

$$q_0 = -0.58 \pm 0.24 \quad , \quad j_0 + \Omega_0 = 0.91 \pm 2.21 \quad , \quad (3.2)$$

The error bars are shrunk by a factor of  $\sim 1.5$ , due to higher accuracy of datasets and more samples at high redshifts. The value of  $q_0$  becomes smaller than that from SNLS data. Meanwhile,  $j_0 + \Omega_0$  moves to a higher value, which is closer to the expected value in the standard flat  $\Lambda$ CDM model, namely  $j_0 + \Omega_0 = 2$  [5].

Finally, we combine the Union compilation and GRB data together to give the constraints in Cosmography I case. We find that with this data combination the mean value of  $q_0$  will become larger, while  $j_0 + \Omega_0$  goes to a smaller value than those of solely SNIa data. The  $1\sigma$  confidence levels are:

$$q_0 = -0.24 \pm 0.19 \quad , \quad j_0 + \Omega_0 = -2.23 \pm 1.37 \quad . \quad (3.3)$$

The constraints have improved significantly.

For the reader's convenience we summarize in Table 1 the constraints on these two parameters from different data combinations.

Data	SNLS		Union	
Parameter	$q_0$	$j_0 + \Omega_0$	$q_0$	$j_0 + \Omega_0$
Best Fit	-0.49	-0.36	-0.58	0.79
Mean	$-0.49 \pm 0.38$	$-0.52 \pm 3.52$	$-0.58 \pm 0.24$	$0.91 \pm 2.21$
$\chi^2_{\min}/\text{d.o.f.}$	117.39/113		317.18/305	
Data	GRB		Union+GRB	
Parameter	$q_0$	$j_0 + \Omega_0$	$q_0$	$j_0 + \Omega_0$
Best Fit	4.47	16.04	-0.23	-2.33
Mean	$4.02 \pm 2.05$	$18.31 \pm 24.86$	$-0.24 \pm 0.19$	$-2.23 \pm 1.37$
$\chi^2_{\min}/\text{d.o.f.}$	74.74/67		402.65/374	

**Table 1:** Constraints on the parameters of Cosmography I from different data combinations ( $1\sigma$  marginalized error bars).

It is interesting to stress that, for every set of data we considered for Cosmography I in Table 1, it is not possible to attribute a definitive sign to the deceleration parameter  $q_0$  up to a confidence level better than the  $2\sigma$  one (a similar issue is also found in [2]).

A further evidence emerging from the data fitting is associated to the relation between  $q_0$  and  $j_0 + \Omega_0$ . In fact, from Fig. 2 it is evident that while SNLS and Union give consistent results (anti-correlated  $q_0$  and  $j_0 + \Omega_0$  parameters), GRB data seems to prefer a relatively strong correlation between  $q_0$  and  $j_0 + \Omega_0$  (albeit they give rather weak constraints).

If confirmed this trend could be an indicator that high redshift data (i.e. those able to breakdown the degeneracy between different dark energy models) are showing a disagreement with the standard models as described by  $\Lambda$ CDM (for which one would instead

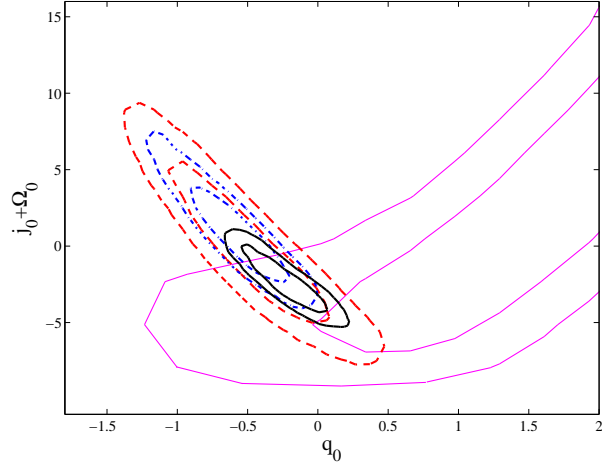


**Figure 2:** Two-dimensional  $1, 2\sigma$  contours of parameters  $(q_0, j_0 + \Omega_0)$  from different data combinations in the Cosmography I case: SNLS (red dashed lines), Union (blue dash-dot lines), Union+GRB (black solid lines) and GRB (magenta thick solid lines). The GRBs now return a correlation in the  $(q_0, j_0 + \Omega_0)$  plane .

expect an anti-correlation). However, an alternative explanation might be given by the fact that the early truncation of the cosmographic expansion characterizing our Cosmography I model is inadequate in properly fitting high redshift data of the GRB type. This feature is also suggested from the fact that the pure GRB data set seems to give rise to a high positive value of  $q_0$ . It is for this reason that we shall now deal with the next order truncation used in the Cosmography II model.

### 3.2 Cosmography II

With the accumulations of different observational data and the improvements of the data quality, it is of great interest to estimate the free parameters in the higher order polynomial terms. In this paper we also try to estimate the snap parameter  $s_0$  from the current data. Here, we still assume flatness ( $\Omega_0 = 1$ ), since the effect of curvature can be safely neglected. In fact, we will find below that the constraint on  $s_0$  is  $\mathcal{O}(100)$ , while the range of curvature should be  $\Omega_0 \sim \mathcal{O}(1)$  which is much smaller than the error bar of  $s_0$ .

In Fig. 3 we show the one dimensional likelihood distributions for  $q_0$  and  $j_0 + \Omega_0$  as obtained from different data combinations.

It is clear for the comparison of this figure with its analogue for Cosmography I, Fig. 1, that in this case we do have a much more regular, and monotonic, improvement in the determination of the cosmological expansion parameters. In particular the use of the Union+GRB dataset does not lead anymore to reversal of the shift of the peak of the likelihood curves towards  $\mathcal{O}(1)$  positive values as it was happening with the model truncated at order  $y^2$  and still gives the best constraints on the three parameters. Furthermore we can now see from the third panel of Fig. 3 that it is only with the addition of the GRBs data that the likelihood peak for the snap parameter  $s_0$  noticeably changes. This is expected as



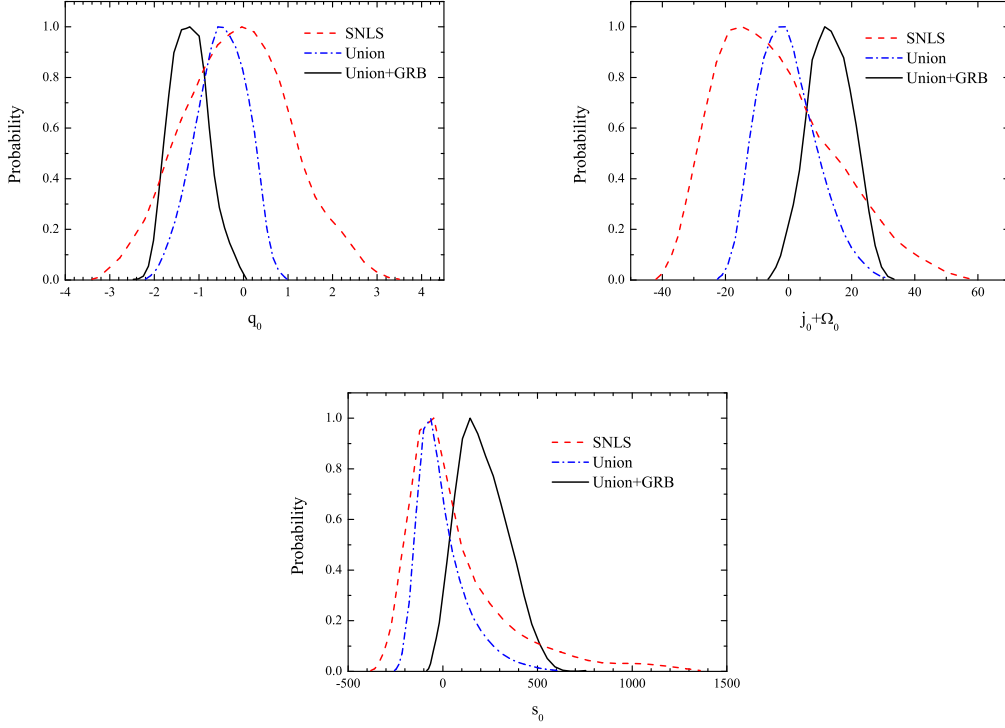


**Figure 3:** One-dimensional likelihood distributions for the parameters  $q_0$ ,  $j_0 + \Omega_0$  and  $s_0$  from different data combinations in the Cosmography II case: SNLS (red dashed lines), Union (blue dash-dot lines) and Union+GRB (black solid lines).

only high redshift data can significantly constraint the higher order in the Hubble expansion (1.10).

In Table II we list the constraints on the parameters from different data combinations when retaining terms up to third order in the polynomial expansion of the logarithmic Hubble relation.

Data	SNLS			Union		
Parameter	$q_0$	$j_0 + \Omega_0$	$s_0$	$q_0$	$j_0 + \Omega_0$	$s_0$
Best Fit	-0.18	-6.42	-86.64	-0.36	-2.97	-61.87
Mean	$-0.12 \pm 1.15$	$-3.51 \pm 18.27$	$72.96 \pm 273.31$	$-0.50 \pm 0.55$	$-0.26 \pm 9.00$	$-4.13 \pm 129.79$
$\chi^2_{\min}/\text{d.o.f.}$	117.32/112			317.07/304		
Data	GRB			Union+GRB		
Parameter	$q_0$	$j_0 + \Omega_0$	$s_0$	$q_0$	$j_0 + \Omega_0$	$s_0$
Best Fit	-2.75	30.54	287.84	-1.26	13.64	211.27
Mean	$0.18 \pm 1.92$	$21.42 \pm 23.32$	$325.31 \pm 336.32$	$-1.22 \pm 0.41$	$13.22 \pm 6.85$	$214.51 \pm 127.84$
$\chi^2_{\min}/\text{d.o.f.}$	72.37/66			395.24/373		

**Table 2:** Constraints on the parameters of Cosmography II from different data combinations ( $1\sigma$  marginalized error bars).

In the case of Union data set improved by the adding of GRBs catalogue, we obtain for the first time a claim for a definitive negative  $q_0$  within (even if marginally)  $3\sigma$ .

It is also interesting to note that now (and in contraposition with Cosmography I) GRB data also favors (as the supernovae ones) an anti-correlation between  $q_0$  and  $j_0 + \Omega_0$ , see Fig. 4. This seems to strongly hint that the previously found  $(q_0, j_0 + \Omega_0)$  correlation in Cosmography I was an artifact of the early truncation in the series (1.10).

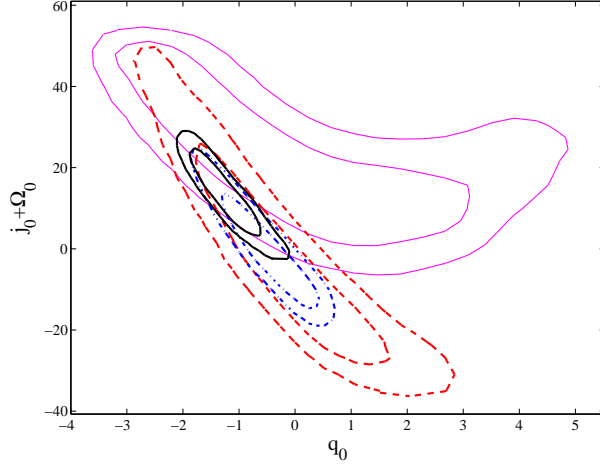


**Figure 4:** Two-dimensional 1, 2  $\sigma$  contours of parameters  $(q_0, j_0 + \Omega_0)$  from different data combinations in the Cosmography II case: SNLS (red dashed lines), Union (blue dash-dot lines), Union+GRB (black solid lines) and GRB (magenta thick solid lines). Now also using GRB data the anti-correlation is maintained.

For completeness we also plot in Fig. 5 the two dimensional contours between  $q_0, j_0 + \Omega_0$  and  $s_0$ . In this case however the errors are still too large for a meaningful comparison with theoretical cosmological solutions such as  $\Lambda$ CDM.

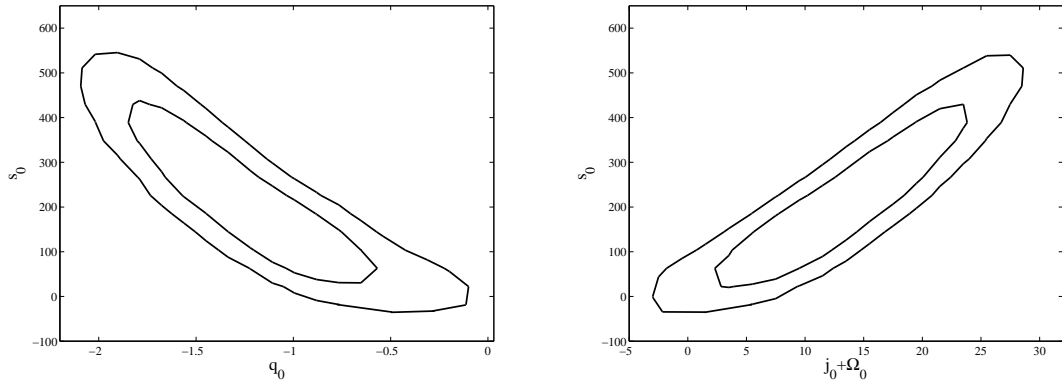


**Figure 5:** Two-dimensional 1, 2  $\sigma$  contours of parameters  $(q_0, s_0)$  and  $(j_0 + \Omega_0, s_0)$  from Union+GRB combination in the Cosmography II case.

### 3.3 Summary

In section 3.1 and 3.2 we carried on the analysis of the Taylor expansion of the luminosity distance in the  $y$ -redshift variable up to second (Cosmography I) and third (Cosmography II) order. In Ref. [2] the authors correctly claimed that keeping the polynomial terms up to the second order is a good approximation to the current SNLS data, since the addition of any further term turns out to be of no statistical relevance.

However, this work shows how a meaningful hope of estimating the snap parameter  $s_0$  becomes a concrete possibility with GRBs. Since we are dealing with the truncation of a series, it is perfectly reasonable that the higher is the redshift reached by data points, the larger is the power of the polynomial we should consider to fit them properly. Actually we have just seen how a early truncation of the series can lead to artifacts such as the  $(q_0, j_0 + \Omega_0)$  correlation in Cosmography I when high redshift data are included.

As a quantitative corroboration to this conclusion we can run, as suggested in [2], a  $F$ -test to establish which is the last relevant term of the expansion we can reach. The  $F$ -test provides a criterion of comparison between two nested models (in our case two successive truncations of a Taylor series), identifying which of two alternatives fits better the data. Supposing that the null hypothesis implies the correctness of the first model, the test verifies the probability to obtain that results fit the alternative hypothesis as well. The less is this probability, the better is the data fitting of the second model against the first one. Quantitatively, one evaluates the  $F$ -ratio among the two polynomials as

$$F = \frac{(\chi_1^2 - \chi_2^2) / (n_2 - n_1)}{\chi_2^2 / (N - n_2)}, \quad (3.4)$$

where  $N$  is the number of data points, and  $n_i$  represent the number of parameters of the  $i$ -model. The  $P$ -value, *i.e.* the area subtended by the  $F$ -distribution curve delimited from the  $F$ -ratio point, quantify the viability of matching models as already mentioned.

While the Cosmography II expansion, with both SNe and GRB, is significantly better than Cosmography I, we explicitly checked that a truncation of the series to the fourth order is not favored, since the decrease of  $\chi^2$  value suggested by an possible Cosmography III is not such to justify the introduction of a new parameter. In conclusion, Cosmography II seems to be currently the most successful scheme for data fitting.

As a final remark let us note that using the Union+GRB dataset the  $\Lambda$ CDM model returns a smaller  $\chi^2$  than the two Cosmographic expansions ( $\chi_{\min}^2/d.o.f. = 390.40/375$ , compared to Cosmography I which is  $\chi_{\min}^2/d.o.f. = 402.65/374$  and Cosmography II which is  $\chi_{\min}^2/d.o.f. = 395.24/373$ ). However, some caution is appropriate here when interpreting  $\chi^2$  values. First,  $\Lambda$ CDM is a solution with one free parameter,  $\Omega_m$ , which is different from those used in the cosmographic expansions (which, moreover, in the case of Cosmography II are three). So the exact statistical significance of the better  $\chi^2$  of  $\Lambda$ CDM might be questionable. Second, if indeed  $\Lambda$ CDM is the solution realized in nature then any approximation to it based on a truncated Taylor series will provide a higher  $\chi^2$  at any redshift (or at most a  $\chi^2$  statistically indistinguishable). Nonetheless, the remarkably good performance of  $\Lambda$ CDM at such high redshift, even with respect to a Cosmographic expansion

with more free parameters (which could hence also reproduce the Hubble expansion of models with a  $z$ -dependent equation of state for dark energy), could be taken as a strong hint in favor of this specific solution.

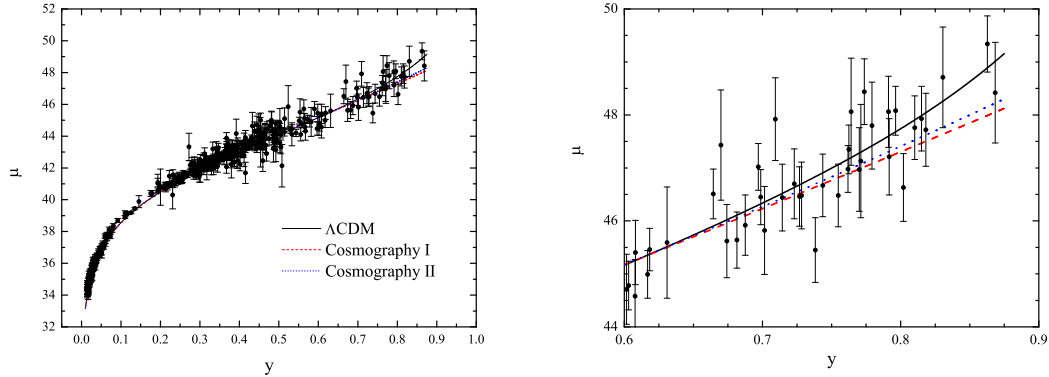


**Figure 6:** Distance moduli for the best-fit values of three cases ( $\Lambda$ CDM, Cosmography I and Cosmography II), together with Union+GRB combination. In the left panel a zoom of the  $0.6 < y < 0.9$  region is presented.

#### 4. Future Perspectives

We want now to present some forecasts for futuristic but realistic mock data sets. For this purpose we have performed an analysis with respect to some fiducial model which is taken as the actual one realized in nature. For concreteness we have taken such a model to be  $\Lambda$ CDM:  $q_0 = -0.55$ ,  $j_0 = 1$  and  $s_0 = -0.35$ .

The projected satellite SNAP (Supernova/Acceleration Probe) would be a space based telescope with a one square degree field of view with  $10^9$  pixels. It aims at increasing the discovery rate for SNIa to about 2000 per year in the redshift range  $0.2 < z < 1.7$ . In this paper we simulate about 2000 SNIa according to the forecast distribution of the SNAP [14]. For the error, we follow the Ref. [14] which takes the magnitude dispersion 0.15 and the systematic error  $\sigma_{\text{sys}} = 0.02 \times z/1.7$ . The whole error for each data is given by:

$$\sigma_{\text{mag}}(z_i) = \sqrt{\sigma_{\text{sys}}^2(z_i) + \frac{0.15^2}{n_i}}, \quad (4.1)$$

where  $n_i$  is the number of supernovae of the  $i$ 'th redshift bin. Furthermore, we add as an external data set a mock dataset of 400 GRBs, in the redshift range  $0 < z < 6.4$  with an intrinsic dispersion in the distance modulus of  $\sigma_\mu = 0.16$  and with a redshift distribution very similar to that of Figure 1 of Ref. [15].

In Table III we list the standard deviations of the free parameters in two different cases. We can find the constraints on the parameters from the future mock data with smaller error bars have improved by a factor of  $\sim 2$ , when comparison with the current

Data	SN	GRB	SN+GRB
$q_0$	0.42	1.11	0.33
$j_0 + \Omega_0$	7.97	11.23	4.92
$s_0$	106.22	90.59	69.16

**Table 3:** The standard deviations,  $1\sigma$  values, of the cosmographic parameters (uncertainties around the best fit value) expected from the future measurements.

constraints. When including  $s_0$ , the constraints will be relaxed by a factor of  $\sim 3$ . Finally, the error of  $s_0$  has been shrunk to 70 by the future SNIa and GRB data. Possibly free parameters in the higher order terms could be estimated by the future measurements, keeping in mind that other potential probes can be used to extract meaningful distance indicators such as the Alcock-Paczynski test using 21 cm at very high redshift ( $z > 10$  e.g. [18]), Baryonic Acoustic Oscillations as measured by BOSS in SDSS-III (e.g [19]), the Alcock-Paczynski for Lyman- $\alpha$  forest ( $z = 2 - 4$ , [20]) and measurements obtained with the shift from the Lyman- $\alpha$  absorption lines ( $z = 1.5 - 4.5$ , [16]).

## 5. Conclusions

Even though the intriguing era of “precision cosmology” has now started, the huge flow of data with increasing resolution is not yet able to solve definitely the contest among different theoretical proposals for the evolution of the universe at late times. The suggestion carried on in this work is a return to a more conservative approach to cosmology, in the meaning of a proper link between observations and cosmographic parameters. In this sense cosmography allows to regain a comprehensive bird’s-eye view on the problem, since it gives an unbiased interpretation to the collected data sets.

We have here included high redshift data ( $z \gtrsim 1$ ) to provide new constraint on the main cosmographic parameters. The lack of validity of the Taylor expansion of the luminosity distance in the usual redshift definition has been circumvented, following the insight of [2], by the translation of the distance definition in a new redshift variable  $y$ , spanning the range  $(0, 1)$  whereas  $z$  runs into the interval  $(0, +\infty)$ ; the improvement obtained with this procedure is that now we are able to fit the data of any possible observable candidate to be a cosmological “standard candle”, no matter what its distance is.

Working with high redshift objects means taking into account both distant SNe (up to  $z \sim 1.55$ ) and GRBs (up to  $z \sim 6.6$ ); in particular, observations of GRBs are quickly approaching even larger redshift (redshifts up to  $z \sim 10$  are expected in next few years). This might make of GRBs the crucial players in the near future, as such high redshifts will allow to determine the higher order parameters of the cosmographic series with unprecedented accuracy. Of course, we do not yet understand GRBs so well that we can use them as proper standard candles. However, it has been proposed to use correlations between GRB observables to standardize their energetics [17]. Furthermore, in this work we have

also use the insight of [10] in order to solve the “circular problem” in the determination of the GRB redshifts.

We performed the calculation for two successive truncations of the Taylor expansion of the luminosity distance (up to the third and fourth order in  $y$ ); further terms are, at the moment, not statistically relevant, as shown by running an F-test. The interest about the possibility to reach the highest possible order is strictly related to the main aim of cosmography: the ability to test and discriminate meaningfully among competing cosmological models. Given that most of the models on the market are build in order to recover (or simulate) Dark Energy at low redshift, their expansion histories are basically degenerate at late times. Breaking such a degeneracy would imply knowledge of the early universe expansion curve and hence would require, within a cosmographic approach, an accurate determination of the higher order parameters jerk  $j_0$  and snap  $s_0$ . This can be achieved only via significant data at high redshift.

Our results can be summarize in few points: we have found that the inclusion of high  $z$  GRB data might lead to misleading results for early truncations of the cosmographic series as in Cosmography I. We showed that the cosmographic series truncated at the fourth order in  $y$ , Cosmography II, is the most accurate and statistically significant one given current data. The latter allows not only a more accurate determination of the lowest order parameters  $q_0$  and  $j_0$  but also a first meaningful estimate of the snap parameter  $s_0$ . All the results are compatible with  $\Lambda$ CDM within  $2\sigma$ . Most importantly, the complete set of Union and GRBs data allows us to introduce for the first time a  $q_0$  definitively negative in the limit of the  $3\sigma$  confidence level.

We have also discussed the future perspective to further ameliorate such results with planned or proposed experiments. In this case we showed that a further reduction of the error bars (by a factor two) will be possible.

## Acknowledgments

We would like to thank Matt Visser for interesting comments and useful suggestions. VV wishes to thank warmly Luca Izzo for fruitful discussions. MV is partly supported by ASI/AAE, INFN-PD51 and a PRIN by MIUR. Part of the numerical computations were performed using the Darwin Supercomputer of the University of Cambridge High Performance Computing Service (<http://www.hpc.cam.ac.uk/>), provided by Dell Inc. using Strategic Research Infrastructure Funding from the Higher Education Funding Council for England.

## References

- [1] C. Cattoen and M. Visser, *Class. Quant. Grav.* **24** (2007) 5985 [arXiv:0710.1887 [gr-qc]].
- [2] C. Cattoen and M. Visser, arXiv:gr-qc/0703122; C. Cattoen and M. Visser, *Phys. Rev. D* **78** (2008) 063501 [arXiv:0809.0537 [gr-qc]].
- [3] S. Weinberg, *Cosmology*, Oxford, UK: Oxford Univ. Pr. (2008)
- [4] M. Visser, *Class. Quant. Grav.* **21** (2004) 2603 [arXiv:gr-qc/0309109v4].

- [5] S. Capozziello and L. Izzo, *Astron. Astrophys.* **490** (2008) 31 [arXiv:0806.1120 [astro-ph]],  
L. Izzo, S. Capozziello, G. Covone and M. Capaccioli, [arXiv:0910.1678 [astro-ph.CO]].
- [6] P. Astier *et al.*, *Astron. Astrophys.* **447**, 31 (2006).
- [7] M. Kowalski *et al.*, *Astrophys. J.* **686**, 749 (2008).
- [8] M. Hicken *et al.*, *Astrophys. J.* **700**, 1097 (2009).
- [9] A. Shafieloo, V. Sahni and A. A. Starobinsky, arXiv:0903.5141 [astro-ph.CO]; H. Wei,  
arXiv:0906.0828 [astro-ph.CO].
- [10] H. Li, J. Q. Xia, J. Liu, G. B. Zhao, Z. H. Fan and X. Zhang, *Astrophys. J.* **680**, 92 (2008).
- [11] C. Firmani, V. Avila-Reese, G. Ghisellini and G. Ghirlanda, *Rev. Mex. Astron. Astrofis.* **43**,  
203 (2007).
- [12] B. E. Schaefer, *Astrophys. J.* **660**, 16 (2007).
- [13] E. Di Pietro and J. F. Claeskens, *Mon. Not. Roy. Astron. Soc.* **341**, 1299 (2003).
- [14] A. G. Kim, E. V. Linder, R. Miquel and N. Mostek, *Mon. Not. Roy. Astron. Soc.* **347**, 909  
(2004).
- [15] D. Hooper and S. Dodelson, *Astropart. Phys.* **27**, 113 (2007).
- [16] J. Liske et al, *Mon. Not. Roy. Astron. Soc.* **386**, 1192 (2008).
- [17] G. Ghirlanda, G. Ghisellini, D. Lazzati, C. Firmani, *Astrophys. J.* **613**, 13 (2004).
- [18] J.-Q. Xia, M. Viel, *JCAP*, **04**, 002 (2009)
- [19] P. McDonald, D.J. Eisenstein, *PhRvD*, 76, 063009, (2007)
- [20] P. McDonald, *Astrophys. J.* **585**, 34 (2003).